IEEE Access
Multidisciplinary | Rapid Review | Open Access Journal

Received December 11, 2021, accepted December 21, 2021, date of publication December 31, 2021,
date of current version January 12, 2022.

Digital Object Identifier 10.1109/ACCESS.2021.3140046

An Optimized Neuro-Bee Algorithm Approach to Predict the FRP-Concrete Bond Strength of RC Beams

AMAN KUMAR[1,2], HARISH CHANDRA ARORA[1,2], MAZIN ABED MOHAMMED[3], KRISHNA KUMAR[4], (Graduate Student Member, IEEE), AND JAN NEDOMA[5], (Senior Member, IEEE)

[1]AcSIR-Academy of Scientific and Innovative Research, Ghaziabad 201002, India
[2]Structural Engineering Department, CSIR-Central Building Research Institute, Roorkee 247667, India
[3]College of Computer Science and Information Technology, University of Anbar, Ramadi 31001, Iraq
[4]Department of Hydro and Renewable Energy, Indian Institute of Technology, Roorkee, Roorkee 247667, India
[5]Department of Telecommunications, Faculty of Electrical Engineering and Computer Science, VSB-Technical University of Ostrava, 70800 Ostrava, Czech Republic

Corresponding author: Jan Nedoma (jan.nedoma@vsb.cz)

This work was supported by the Ministry of Education of the Czech Republic under Project SP2022/18 and Project SP2022/34.

ABSTRACT Over the world, there is growing worry about the corrosion of reinforced concrete structures. Structure repair, rehabilitation, replacement, and new structures all require cost-effective and long-lasting technologies. Fiber Reinforced Polymer (FRP) has been widely employed in both retrofitting existing structures and building new ones. Due to its varied qualities in reinforced concrete and masonry constructions as a repair composite material, FRP have seen a rise in use over the last decade. This material have several advantages such as high stiffness-to-weight and strength-to-weight ratios, light weight, possibly high longevity, and relative ease of usage in the field. Among all the parameters the bond between concrete and FRP composite play an important role in the strengthening of structures. However, the bond behaviour of the FRP-concrete interface is complex, with several failure modes, making the bond strength difficult to forecast, resulting in the FRP strengthened concrete structure. To overcome such kind of issues machine learning models are sufficient to forecast the bond strength of FRP-concrete. In this article Artificial Neural Network (ANN), optimized Artificial Bee Colony (ABC)-ANN and Gaussian Process Regression (GPR) algorithms are deployed to predict the bond strength. The R-value of ABC-ANN and GPR models are 0.9514 and 0.9618 respectively. This research aids researchers in estimating bond strength in less time, at a lower cost, and with less experimental work.

INDEX TERMS ABC-ANN, ANN, bond strength, FRP-concrete bond, FRP, machine leaning.

I. INTRODUCTION

Repairing deteriorating, damaged, and deficient civil infrastructure has become a major concern for civil engineers all around the world [1]. The rehabilitation of old structures is rapidly expanding, particularly in wealthy countries that finished the majority of their infrastructure in the mid-nineteenth century [2]. Furthermore, post-World War II constructions gave little consideration to durability concerns, and the United States and Japan lacked understanding of seismic design [3]. Chloride-induced corrosion of steel reinforcements is one of the most prevalent causes of deterioration in reinforced concrete (RC) structures [4]. Reinforcement corrosion reduces the structural performance and service life of RC structures, and affects life-cycle cost of RC structures rises as a result of the maintenance and repair interventions required to address this problem. This issue is particularly serious in some developed countries, where RC infrastructure components have been in use for decades [5], [6]. Reinforcing steel corrosion may create cracks in the surrounding concrete owing to the expansion pressure generated during the production of corrosion products, in addition to the loss of effective cross-sectional area of the reinforcing steel [7], [8]. The concrete cover may potentially spall as a result of the expansion pressure. In general, such degradation reduces the load carrying capacity of the RC member's or structures

The associate editor coordinating the review of this manuscript and approving it for publication was Wai-Keung Fung.

and its stiffness [9]–[11]. The escalation of environmental contamination in recent decades has resulted in a substantial increase in corrosion phenomena in RC structures, which has resulted in several collapses, particularly in those structures that have not received appropriate maintenance. [12]–[16]. The Swiss Federal Laboratory for Materials Testing and Research (EMPA) originally investigated this approach of reinforcing RC beams in the mid-1980s, although much of the research on FRP plate bonding for flexural strengthening has taken place in the last 20 years [17].

The Hyogoken–Nanbu earthquake struck Kobe, Japan, in 1995, causing widespread devastation [18]. As a result, the Japan Building Disaster Prevention Association (JBDPA, 1999) released the Seismic Retrofitting 'Design and Construction Guidelines for Existing RC bridges using Fibre FRP Materials' in September 1999 [19]. As a result, cost-effective and long-lasting solutions are required for concrete structure repair, rehabilitation, replacement, and new construction [20]. Building construction and maintenance might benefit from advanced FRP composite materials [21]. The advanced polymer composite is a hybrid material made up of two major components: fibre and polymer [22]. The fibres have high strength and modulus while matrix material or polymer have low modulus and strength [23]. The fibre uses the matrix's plastic flow to transmit burden/load to the fibre under stress, resulting in a high-modulus and strength composite [24]. The high aspect ratio fibres in the primary phase must be properly distributed and bound with the matrix in the secondary phase. As a result, the fibre, matrix, and interface are the three main components of the composite [25]. To optimize the coupling between the two phases and therefore allow stresses to be dispersed over the matrix and hence transferred to the reinforcement, the interface between the fibre and the matrix must have sufficient chemical and physical bonding stability [26].

FRP has been widely used in civil structure strengthening as a composite material with eminent characteristics [27]. FRP offers several advantages, including corrosion resistance, long durability, and ease of construction, making it one of the finest materials for concrete structure rehabilitation [28]. Bonding is an essential factor in shear and flexural strengthening systems of RC structures. External Bonded FRP (EBF) is the most often used approach for reinforcing existing RC components; nevertheless, despite its simplicity of use, the EBR technique's performance can be significantly harmed by different forms of delamination/debonding of FRP composite from concrete substrate [29].

In concrete sections reinforced with FRP material, the fracture generally begins in the concrete substructure near the FRP strip, and therefore the mechanical properties and failure of the concrete play a major role in retrofitting efficiency. In addition to bond length, FRP strip width, axial stiffness, and its ratio to concrete element width all impact the FRP concrete bond strength [30]. In order to determine the FRP-concrete bond strength, numerous investigational studies have been accompanied to examine the effect of various parameters for both concrete and FRP composite material including adhesive properties [31]. Afterwards on the basis of these investigational and theoretical analysis, several analytical prediction models were developed and implemented in appropriate repair and rehabilitation codes such as fib bulletin [32], Italian National Research Council CNR-DT200/2004 [33], ACI [34], HB305 [35] and CS-TR-55-UK [36].

The majority of these analytical models were developed based on the restricted experiment data, which predict the bond strength in a specific group of data samples, but for other set of data samples the accuracy of the model may be differ depending on the properties of concrete and FRP composite material. Because of the complexities in the offered analytical approaches and the majority of the numerical models given, they are unable to assess the true debonding behaviour. As an alternative and complementary approach, Multiple-linear Regression (MLR) methods are used for predicting bond behaviour: computational methods such as ANN, FL, SVM, FIS, GP, ANFIS, and GEP.

Metaheuristics are well-suited to combinatorial optimization issues because they can frequently discover a satisfactory solution in a reasonable period of time. As a result, they are a viable alternative to exhaustive search, which would require more time. Meta-heuristics are not problem-specific, they may be applied to a wide range of issues. Like, genetic algorithms are used in many possible problems, although they may not always be the best solution to each of these problems. The ABC method is relatively resilient, converges quickly, has a small number of parameters, and is very adaptable.

There are several studies reported in the literature that employed hybrid ANN models in civil engineering applications, and some of them are: Sarir *et al.* [37] used whale optimization and gene expression programming (GEP) tree-based to calculate the bearing capacity of concrete filled steel columns. The GEP tree-based models shows the better performance among all the models ($R^2$of Training and testing was 0.928 and 0.939 respectively). The accuracy of PSO-ANN model in terms of coefficient of determination was found as 0.910 and 0.904 for training and testing data respectively. Mansour *et al.* [38] explored the Neuro-Swarm algorithms to predict the pile settlement. The predicted results reveal that the neuro-swarm model has high accuracy up to a coefficient of determination of 0.892. Apostolopoulou *et al.* [39] and Sun *et al.* [40] used ANN and hybrid ABC-ANN to predict and optimized the compressive strength of mortar and concrete samples. Performance of FRP-concrete bond strength by utilizing the ANN and ABC-ANN was evaluated by Jahed *et al.* [41]. When compared to the ANN model, the anticipated results suggest that ABC-ANN can perform better. The author only employed 150 samples in his dataset, which limits the model's usefulness.

Paji *et al.* [42] investigated the compressive strength behaviour under fresh and magnetic salty water with machine learning models such as neuro-swarm and neuro-imperialism. The training and testing results present the better performance of neuro-swarm optimized algorithm. MLP-GWO

(multilayer perceptron - gray wolf optimization) and ANFIS-GWO (adaptive neuro-fuzzy inference system - gray wolf optimization) models were used to calculate the bearing capacity of the piles by Dehghanbanadaki *et al.* [43]. The results demonstrated that both the MLP and ANFIS approaches were capable of accurately predicting the piles' ultimate bearing capacity. But, MLP-GWO model provided better results in terms of R^2-value 0.991 for test data. Khari *et al.* [44] used hybrid neuro-swarm method to forecast the lateral defection of piles. In the lateral deflection prediction process, the suggested PSO–ANN model was proven to be capable of giving high accuracy while also having a low system error. The value of coefficient of determination of training and testing data were 0.953 and 0.944 respectively. Asteris *et al.* [45] used only ANN to predict the shear strength of RC beams. Momeni *et al.* [46] worked on ANN model with two optimizing algorithms, Gravitational Search Algorithm (GSA) and PSO to forecast the deformation of geogrid-reinforced soil structures. The results of both the GSA-ANN and PSO-ANN models were good enough. However, GSA-based ANN prediction model outperforms, with a R-value of 0.981 and a system error of 0.0101 for testing data.

Liao *et al.* [47] optimized the ultimate axial load of circular concrete-filled steel tubes using fuzzy-based approach. Two hybrid models firefly algorithm (FFA) and differential evolution (DE) were used to optimize the conventional fuzzy systems (FS). Both FFA-FS and DE-FS enhance accuracy above analytical models by 9.68 percent and 6.58 percent, respectively, according to prediction findings. Mohammed *et al.* [48] used neuro-imperialism and neuro-swarm models to forecast the fly ash added compressive strength of concrete. The neuro-swarm and neuro-imperialism models have train and test R-values of (0.9042 and 0.9137) and (0.8383 and 0.8777), respectively. Although both strategies are capable of performing prediction tasks, the results show that the proposed neuro-swarm model is a better alternative technique for mapping concrete strength behaviour.

These computational algorithms each have their own structure, as well as various strengths and limitations. It has been demonstrated that their regression abilities are limited [49]. Many researches in the past already done their work in the bond prediction behaviour, but as a consequence, the prediction model established on them is still incomplete and requires additional development.

To accurately design and simulate buildings using FRP composite materials, it is critical to use an accurate and efficient model for forecasting the bond strength of FRP-concrete. In the proposed work, both optimized ABC-ANN and GPR models have been deploy to calculate the FRP-bond strength of RC beams. Researchers will be able to use the findings of this study, to calculate the FRP-bond strength with greater precision and less experimentation work. The main limitations of this work is that a user can only use the proposed model of this article for an input vector that be within the interval of each input variable.

The work in this paper is divided into seven part. First section deals with the basic information of the degradation of concrete structures, rehabilitation, FRPs and machine learning approaches. In the second section the data related to FRP-concrete bond was collection from the literature and the performance indices used to evaluate the accuracy of this study. In third section, the previously used analytical models were collected and separates into two parts (i) codal models and (ii) models. Codal model are used in the internationally known standards such as Fib, ACI, HB 305 etc. and simple models are directly extracted from the previous articles and used by numerous authors. Section 4 introduces the ANN, ABC-ANN And GPR models. Section 5 deals with the compression of machine learning models with analytical models. In section 6, the proposed formula derived from ABC-ANN is described. The conclusion and future scope are mentioned in the last section.

II. COLLECTION OF DATA

Currently there is no appropriate code for the experimental investigation of FRP-concrete bond strength, and prior studies have only established a few traditional test configurations, such as beams bending tests, single and double shear tests. The bond strength testing setup is depicted in Figure 1. The collected database contains both single and double shear 744 samples results [29], [50]–[76] and parameters which includes f_c' is the concrete with specified compressive strength (MPa), b_f is the width of the FRP laminate/fabric (mm), E_f is the modulus of elasticity of FRP material (GPa), t_f is the thickness of FRP material (mm), b_c is the width of concrete block (mm), f_f is the tensile strength of FRP composite (MPa) and L_b (mm) is the length FRP bonded material are tabulated in Table 1. Table 2 shows the statistical features of each major component in the database.

Figure 2 depicts the frequency classification of test data collected from the literature, represent the different parameters of concrete and FRP composite specimens, such as compressive strength of concrete (f_c'), width of concrete block (b_c), modulus of elasticity of FRP material (E_f), tensile strength of FRP material (f_f), thickness of FRP material (t_f), is the width of the FRP laminate/fabric (b_f) and (L_b) is the length FRP bonded material.

III. PREDICTION OF BOND STRENGTH USING EXISTING ANALYTICAL FORMULATION

Presently, numerous analytical models for determine the bond strength of FRP-concrete have been established, with varying degrees of success. Some of the most important adopted codes in the world recognized association such as ACI, fib bulletin and HB305 were also used to predict the bond strength.

A. CODAL STANDARDS TO PREDICT THE BOND STRENGTH

(a) Codal Model 1 - The first model which is selected in fib Bulletin [32] was given by Neubauer and Rostasy [77] (1997)

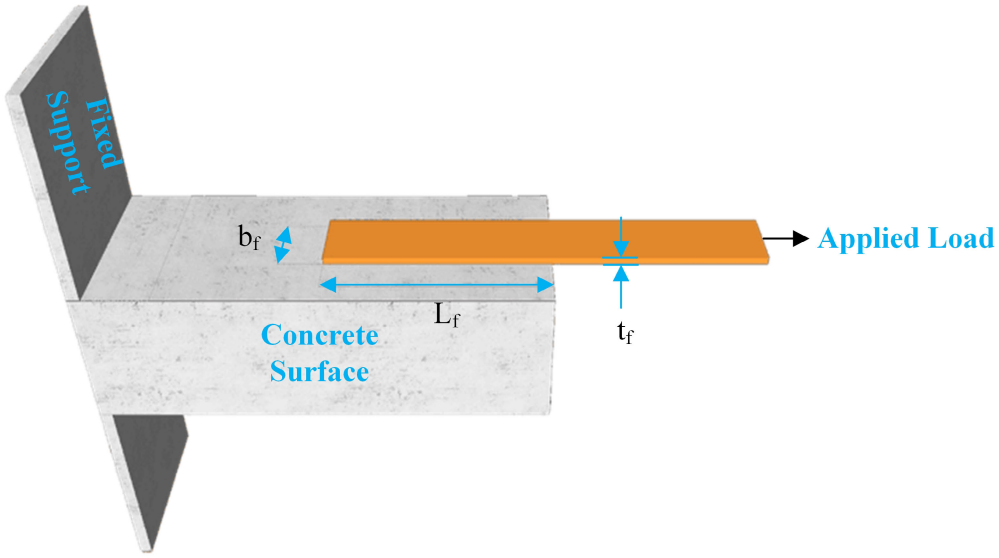

FIGURE 1. Arrangement of bond strength test setup.

TABLE 1. Parameters for bond strength analysis from collected database.

Reference	f'_c (N/mm^2)	b_c (mm)	E_f (GPa)	f_f (N/mm^2)	t_f (mm)	b_f (mm)	L_b (mm)	P_u (kN)
Chajes et al. [50]	24-471	115-229	108.38	234-5172	1.02	25.4	50.8-203.2	8.1-12.81
Maeda et al.[51]	40.8-44.7	100	230-80	5000	0.5	65	700	5.8-16.25
Täljsten et al. [52]	29.7-65.8	100-200	170-300	3792-6700	1.2	50	100-400	17.3-45.95
Ueda et al. [53]	23.5-46.5	100-500	230-372	3792	0.11-0.55	10-100	65-700	2.4-38
Zhao et al. [54]	16.2-29	150	240	3792	0.08	100	100-150	11-12.75
Wu et al. [55]	46.5-58.3	100	23.9-390	3792	0.08-1	40-100	250-300	11.8-27.25
Adhikary et al. [56]	24-36.5	150	230	3792	0.11-0.33	100	100-150	16.75-28.5
Fu-quan et al. [57]	24.1-70	100	230	3792	0.17-0.84	30-70	50-300	7.831.13
Nakaba et al. [58]	23.8-57.6	100	124.5-425.1	3792	0.17-0.19	50	300	8.9-26.78
Tan [59]	29.7	100	97-235	3792	0.11-0.34	50-75	70-130	6.46-13.95
Dai et al. [60]	33.1-35	100	74,83.60, 230	1550-3550	0.11-0.381	100	330	15.6-64.8
Ren [61]	22.7-43.8	150	83.03-207	3792	0.33-0.51	20-80	60-150	4.61-22.8
Yao et al. [62]	18.9-27.1	100-150	256	3792	0.17	15-100	75-240	3.81-19.07
Dai et al. [63]	35	200	74,84,230	1550-3550	0.11-0.38	100	330	13.5-60.9
Sharma et al. [64]	29.7-35.8	100	165-300	3792	1.2	50	100-300	18.25-46.35
Toutanji et al. [65]	17-61.5	200	110	4100	0.5-0.99	50	100	7.56-19.03
Yun and Wu [66]	36.9-48.6	150	230	3400	0.167	50	300	3.2-27.7
Ceroni et al. [67]	15-20	250	80.70-230	2560-4830	0.166-0.48	100	200-300	12.52-22.81
Hosseini et al.[29]	36.5-41.1	150	238	4300	0.131	48	20-250	7.54-10.12
Li et al. [68]	27-61	100	270	3500	0.167	50	50-300	11.03-20.87
Ueno et al. [69]	23-74.5	80	42.66-43.54	1995-2000	1.03-1.8	40	200-230	9.52-18.29
Chen et al. [70]	42-72	100	242	3513	0.167	50	300	8-22.21
Yuan et al. [71]	39.68-50.98	150	73	1333	0.12	40	200	10.12-12.96
Mosto. et al. [72]	24.7-40.4	150	230	3900	0.166	50	200	10.2-14.98
Mofrad et al. [73]	20-43	150	230, 238	3900,4300	0.131-0.26	48	150	10.54-27.3
Zhang et al. [74]	29.3	100	256	4100	2	20	150-180	7.53-9.27
Yuan et al. [75]	30.14	150	73-210	1400-2450	0.12-0.287	40	200	3.73-17.66
Mogh. et al. [76]	22.7-48.2	150	76-230	2300-3900	0.11-0.34	30-60	200	3.9-24.5

is expressed below:

$$P_u = \begin{cases} 064\, k_p b_f \sqrt{0.53 E_f t_f \left(f'_c\right)^{0.5}}, & L_b \geq L_e \\ 0.64 \dfrac{L_b}{L_e}\left(2 - \dfrac{L_b}{L_e}\right) k_p b_f \sqrt{0.53 E_f t_f \left(f'_c\right)^{0.5}}, & L_b < L_e \end{cases} \tag{1}$$

where, k_p is the geometric factor and calculated using below formula. L_e is the effective length calculated using equation 3.

$$k_p = \sqrt{\frac{1.125\left(2 - \frac{b_f}{b_c}\right)}{1 + \frac{b_f}{400}}} \geq 1 \tag{2}$$

$$L_e = \sqrt{\frac{E_f t_f}{1.06\left(f'_c\right)^{0.5}}} \tag{3}$$

(b) Codal Model 2 - To predict the bond strength Chen and Teng [78] (2001) model which was adopted by ACI 440. R-08 [34]. The formula for model prediction is shown below:

$$P_u = 0.427 \beta_p \beta_L \sqrt{f'_c} L_e b_f \tag{4}$$

where, P_u = applied load (kN), β_p and β_L are the geometric parameters, f'_c is the concrete with specified compressive strength (MPa), L_e is the effective length (mm) and b_f is the width of the FRP laminate/fabric.

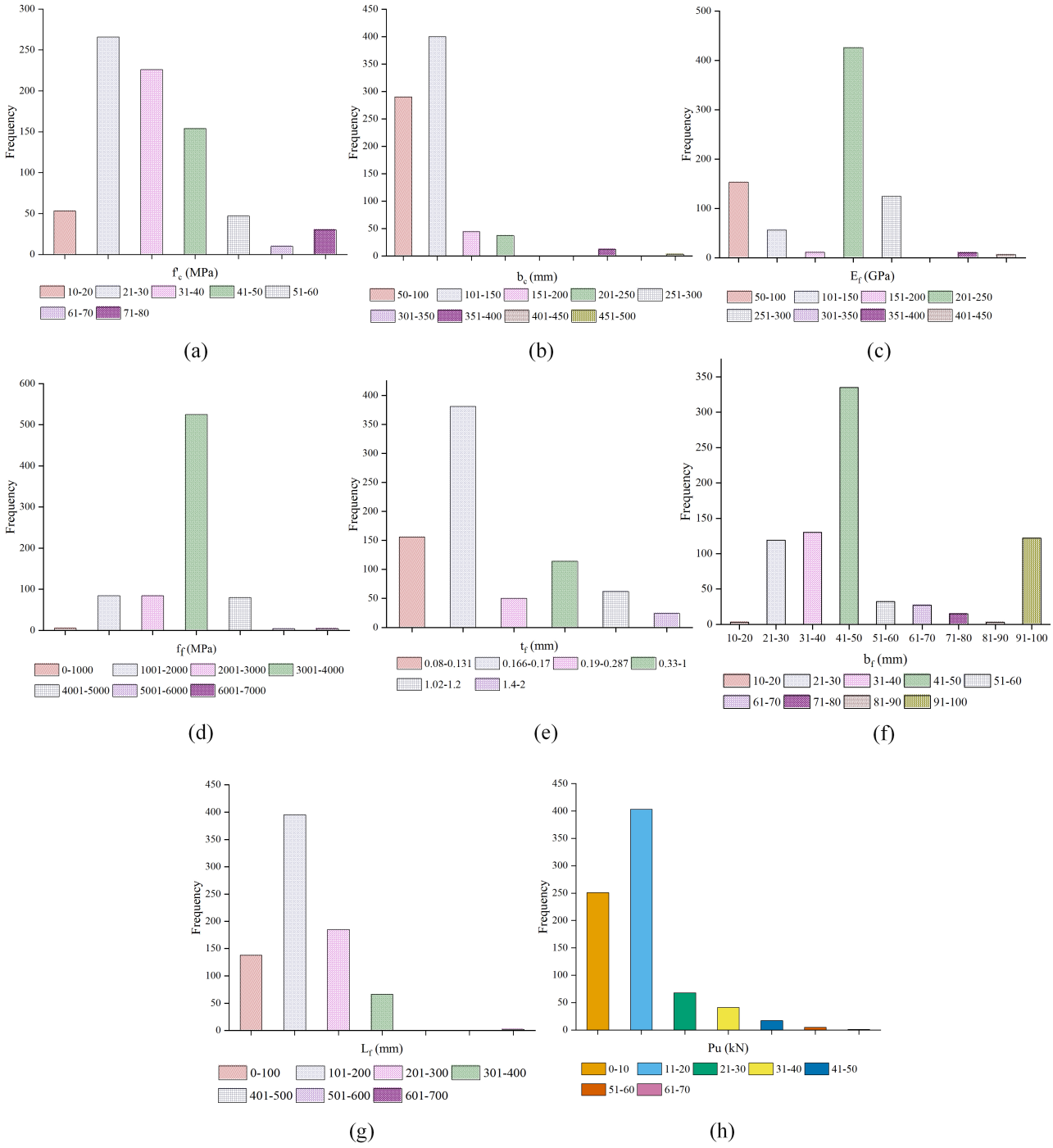

FIGURE 2. Distribution of the inputs and output variables (a) Input 1 f_c' (b) Input 2 b_c (c) Input 3 E_f (d) Input 4 f_f (e) Input 5 t_f (f) Input 6 b_f (g) Input 7 L_b (h) Output P_u.

The geometric parameter β_p, β_L and effective length is calculated using below expressions:

$$L_e = \sqrt{\frac{E_f t_f}{\sqrt{f_c'}}} \tag{5}$$

$$\beta_p = \left[\frac{2 - \frac{b_f f}{b_c}}{1 + \frac{b_f}{b_c}}\right]^{0.5} \tag{6}$$

$$\beta_L = \begin{cases} 1, & L \geq L_e \\ \sin\left(\frac{\pi L_b}{2L_e}\right), & L < L_e \end{cases} \tag{7}$$

where, E_f is the modulus of elasticity of FRP material (MPa), t_f is the thickness of FRP material (mm), b_c is the width of concrete block (mm) and L_b is the length FRP bonded material.

TABLE 2. Statistical features of each major component in the database.

Parameters	Symbol	Unit	Min.	Max.	Mean	Std.	Kurtosis	Skewness	Type
Concrete	f'_c	(N/mm^2)	15	74.5	36.63	12.68	3.78	0.95	Input
	b_c	(mm)	80	500	142.97	55.13	15.3	2.83	Input
	E_f	(GPa)	23.9	425.1	199.03	76.49	3.10	-0.59	Input
	f_f	(N/mm^2)	234	6700	3440.86	875.20	4.21	-0.80	Input
	t_f	(mm)	0.08	2	0.33	0.37	8.29	2.42	Input
	b_f	(mm)	10	100	53.94	22.93	3.03	0.95	Input
	L_b	(mm)	20	700	206.99	82.17	5.06	0.49	Input
P_u		(kN)	2.4	64.8	15.64	9.26	7.51	1.91	Output

(c) Codal Model 3 - The fourth FRP bond prediction model is given by Italian National Research Council CNR-DT 200/2004 [33] is expressed as:

$$P_u = \begin{cases} b_f \sqrt{2E_f t_f k_f}, & L_b \geq L_e \\ b_f \sqrt{2E_f t_f k_f} \dfrac{L_b}{L_e}\left(2 - \dfrac{L_b}{L_e}\right), & L_b < L_e \end{cases} \tag{8}$$

where, k_f is the specific fracture energy and calculated using following formula:

$$k_f = 0.03 k_b \sqrt{f'_c f_c} \tag{9}$$

$$k_b = \sqrt{\frac{2 - \frac{b_f}{b_c}}{1 + \frac{b_f}{400}}} \geq 1 \tag{10}$$

$$L_e = \sqrt{\frac{E_f t_f}{2 f_c}} \tag{11}$$

where, f_c is the mean value of concrete tensile strength.

(d) Codal Model 4 - Seracino *et al.*'s [79] FRP bond prediction model is presented in the HB 305 (2007) [35] standard. The formula given by the authors is expressed as:

$$P_u = 0.853 \beta_a \left(f'_c\right)^{0.33} \left(\frac{d_f}{b_f}\right)^{0.25} \sqrt{\left(2d_f + b_f\right) E_f b_f t_f} \tag{12}$$

where, d_f = thickness of the failure plane and β_a is the range of values as expressed in below equation:

$$\beta_a = \begin{cases} 1, & L_b \geq L_e \\ \dfrac{L_b}{L_e}, & L_b < L_e \end{cases} \tag{13}$$

$$L_e = \frac{\pi}{2\sqrt{\frac{\tau_f \left(2d_f + b_f\right)}{\delta_f^E f b_f t_f}}} \tag{14}$$

where, τ_f is the peak interface shear stress and δ_f = slip at maximum interface shear stress calculated using below expression:

$$\tau_f = \left(0.802 + 0.078 \frac{d_f}{b_f}\right) \left(f'_c\right)^{0.6} \tag{15}$$

$$\delta_f = \frac{0.73 \left(\frac{d_f}{b_f}\right)^{0.5} \left(f'_c\right)^{0.67}}{\tau_f} \tag{16}$$

(e) Codal Model 5 - The fifth model is given by the Concrete Society Committee CS-TR-55-UK [36] can be expressed as:

$$P_u = \begin{cases} 0.5\, k_b b_f \sqrt{E_f t_f f_{ct}}, & L_b \geq L_e \\ 0.5\, k_b b_f \sqrt{E_f t_f f_{ct}} \dfrac{L_b}{L_e}\left(2 - \dfrac{L_b}{L_e}\right), & L_b < L_e \end{cases} \tag{17}$$

where, $f_c t$ is the characteristic axial tensile strength of concrete, k_b and L_e are calculates using equations:

$$k_b = 1.06 \sqrt{\frac{2 - \frac{b_f}{b_c}}{1 + \frac{b_f}{400}}} \geq 1 \tag{18}$$

$$L_e = 0.7 \sqrt{\frac{E_f t_f}{f_{ct}}} \tag{19}$$

B. MODELS OTHER THAN CODAL STANDARDS

(a) Model 1 = Sato *et al.* (1997) [80] and Japan Concrete Institute (2003) [81] suggested a model to predict the FRP bond strength using following equations:

$$P_u = k L_e \left(b_f + 7.4\right) \tag{20}$$

$$\mathrm{k} = \left(2.68 \times 10^{-5}\right) \left(f'_c\right)^{0.2} E_f t_f \tag{21}$$

$$L_e = 1.89 \left(E_f t_f\right)^{0.4} \quad \text{if } L_b \geq L_e \tag{22}$$

where, P_u = bond strength (kN), b_f = width of FRP laminate/fabric, E_f is the modulus of elasticity of FRP material (MPa), t_f is the thickness of FRP material (mm), L_e is the effective length (mm).

(b) Model 2 - Khalifa *et al.* (1998) [82] suggested a model to predict the FRP bond strength using equation:

$$P_u = k L_e b_f \tag{23}$$

k and L_e is calculated using equation 24 and equation 25 respectively.

$$\mathrm{k} = \left(110.2 \times 10^{-6}\right) \left(\frac{f'_c}{42}\right) E_f t_f \tag{24}$$

$$L_e = e^{6.134 - 0.58 \ln\left(E_f \cdot t_f\right)} \tag{25}$$

(c) Model 3 - Maeda *et al.* (1999) [83] proposed a model to predict the FRP bond strength using equation:

$$P_u = k L_e b_f \tag{26}$$

k and L_e is calculated using equation 27 and equation 28 respectively.

$$\mathrm{k} = \left(110.2 \times 10^{-6}\right) E_f t_f \tag{27}$$

$$L_e = e^{6.134 - 0.58 \ln\left(E_f \cdot t_f\right)} \tag{28}$$

(d) Model 4 - Yang *et al.* (2007) [84] proposed a model to predict the FRP bond strength using equation 29.

$$P_u = \left(0.5 + 0.08\sqrt{\frac{0.01 E_f t_f}{f_f}}\right) b_f L_e \mathrm{k} \tag{29}$$

where, f_f is the tensile strength of FRP material in (MPa) and $L_e = 100$ mm.

$$k = 0.5 f_f \tag{30}$$

IV. ARTIFICIAL INTELLIGENCE TO PREDICT FRP-CONCRETE BOND STRENGTH

To predict the bond strength in this used algorithms are ANN, ANN-ABC and multiple linear regressions.

A. ARTIFICIAL NEURAL NETWORK (ANN)

ANNs are one of the most commonly utilized approaches in the field of artificial intelligence (AI). These techniques are simple, have excellent performance, and have a cheap computational cost [85]. In the literature, there are several varieties of ANNs, including Spiking Neural Networks (SNN), Feed-forward Neural Networks (FFNN), Kohonen self-organizing feature map networks (SOM), Recurrent Neural Networks (RNN), and Radial basis function networks (RBF) [86]. The FFNN is the most commonly used and simplest of all ANNs. FFNNs use one-way connections between neurons in various layers to accept information as inputs on one side and produce outputs on another side [87]. FFNNs are classified into two types: Single-Layer Perceptrons (SLP) and Multi-Layer Perceptrons (MLP). There is only one perceptron in SLPs. SLPs, despite their simplicity, are incapable of dealing with non-linear issues. As a result, MLPs with more than one perceptron built in various layers are used [88], [89].

In MLP's primary components are the input layer, hidden layer(s), and output layer. The hidden layer contains the activation function, weights, and units (or neurons). Without performing any computational calculation, the input layer takes information from the outer context and transmits it to hidden layers neurons. The majority of a network's internal processing is performed by hidden layers, which are sandwiched in the input and output layers. Finally, the output layer is in charge of delivering network computations to the outside world. The activation function describes how the neurons process the input value to create the output value for the succeeding layer, and the subsequent layers are fully linked by weight.

Data normalization was done before to training the network in order to reduce undesired feature scaling effects and provide higher computational stability. All parameters were converted linearly in accordance with equation 31 and the Log-sigmoid [90]–[95] activation function detect values in the interval [0, 1]. The normalization process is quantitatively expressed as follows.

$$x^* = \frac{(x - x_{\min})}{x_{\max} - x_{\min}} \tag{31}$$

where x^* = normalizing value, x = original value, x_{max} = upper value in the selected data set, and x_{min} is the lower value in the selected data set.

$$\mathrm{TanSig} = \frac{2}{1 + e^{-2x}} - 1 \tag{32}$$

Artificial neural networks (ANNs) were trained and evaluated using the MATLAB R2021a (MathWorks, 2021) programme [96]. To train the proposed network in MATLAB, the feed-forward back propagation method using the Levenberg-Marquardt (LM) algorithm was used. The use of a single hidden layer to handle several nonlinear problems has been validated in the literature. Throughout this layer-by-layer training process, the input signals were sent forward, while the error signals were sent back. The weights were continually changed until the output layer gave the desired output. 744 dataset points were divided into three groups on the random basis. For training, validation, and testing, 520 data (70 percent), 112 data (15 percent), and 112 data (15 percent) were acquired, respectively. In the network training process the training and validation sets were employed, while the test and training sets were used to evaluate network performance.

Five frequently used performance indices, including mean absolute error (MAE), coefficient of determination R-squared (R^2), correlation coefficient (R), root mean squared error (RMSE), mean square error (MSE) and mean absolute percentage error (MAPE) are used to measure the performance of each FRP bond strength prediction model. These indexes' relevant expressions are in equation 33 to equation 37. Additionally, a20-index is also used to measure the performance of each model and mentioned in equation 38.

$$R^2 = 1 - \left(\frac{\sum_{i=1}^{N} (a_i - p_i)^2}{\sum_{i=1}^{N} p_i^2}\right) \tag{33}$$

$$RMSE = \sqrt{\frac{1}{N}\sum_{i=1}^{N} (a_i - p_i)^2} \tag{34}$$

$$MAE = \frac{\sum_{i=1}^{N} |a_i - p_i|}{N} \tag{35}$$

$$MSE = \frac{1}{N}\sum_{i=1}^{N} (a_i - p_i)^2 \tag{36}$$

$$MAPE = \frac{1}{N}\left|\frac{\sum_{i=1}^{N} |a_i - p_i|}{\sum_{i=1}^{N} |a_i|}\right| \times 100 \tag{37}$$

$$a20 - \text{index} = \frac{m20}{N} \tag{38}$$

where, N is the number of points in the data set, and a and p sets are the actual and projected output sets, respectively.

m20 is the number of samples with values rate measured/predicted value (range between 0.8-1.2).

Researchers have used trial and error techniques to identify the optimum number of neurons and the suitable ANN. In this study, 2 to 24 number of neurons were used to define the optimum ANN architecture. To determine the optimum network design, traditional statistical errors and performance metrics, such as MSE and R, were utilized. As a result, the evaluation index (R, MSE) of each pattern is calculated and the outcomes are determined in line with the competence of the responses. Finally, calculate the rank for each of the proposed patterns and the optimum architecture of the network is chosen. The outcomes in the assessment of bond strength in artificial neural network are shown in Table 3.

As indicated in Table 3, the 19 neurons was identified as the best network among all the neurons based on the ranking systems. Figure 3 provides a schematic overview of the selected neural P_u estimating networks. The values of the correlation coefficients (R) and MSE in the selected network for training and testing analysis are 0.97094 and 0.9378 and notably small values 0.00105 and 0.00262 respectively. These data demonstrate the optimized artificial neural network's strong capabilities for calculating the bond strength. Although validation of numerical findings is not always included in artificial intelligence-based studies, there have been numerous examples described in the literature where the model dataset is created using numerical modelling without validation [46], [94].

B. ARTIFICIAL BEE COLONY - ARTIFICIAL NEURAL NETWORK (ABC-ANN)

For dealing with restricted optimization issues, many deterministic and stochastic methods have been developed. Deterministic methods, such as Feasible Direction [98] and Generalized Gradient Descent [99], involve significant assumptions on the objective function's continuity and differentiability. As a result, their applicability is restricted because these qualities are rarely seen in real-world issues. Stochastic optimization methods, such as Particle Swarm Optimization (PSO), Genetic Algorithms (GA), and Evolutionary Programming do not make such assumptions and have been effectively utilized for solving restricted optimization issues in recent years [100]. For numerical optimization challenges, Karaboga developed an Artificial Bee Colony (ABC) method based on honey bee foraging behavior [101]. Karaboga and Basturk evaluated the performance of the ABC method on unconstrained problems to that of other well-known contemporary heuristic algorithms such as Particle Swarm Optimization (PSO), Genetic Algorithm (GA) and Differential Evolution (DE). The ABC method is extended to solve constrained optimization (CO) problems.

One of the most prominent swarm-based heuristic optimization methods is the ABC algorithm. It comprises three sorts of bees: employed bees, onlooker bees, and scout bees. The ABC algorithm makes several assumptions. Among these are: half of the colony is made up of employed bees and other half consists of onlooker bees [96]. The number of employed bees is exactly equal to the number of onlooker bees. The following are the basic steps of the ABC algorithm:

The ABC creates a randomly dispersed starting population of SN solutions (food sources), where SN represents the size of the swarm. Let $x_i = x_{i_1}, x_{i_2}, \ldots, x_{i_n}$. x_i shows the i_{t_h} solution in the swarm. Each employed bee x_i creates a new applicant solution V_i in its near area, as mentioned in equation 39.

$$v_{i,j} = x_{i,j} + \phi_{i,j} \times \left(x_{i,j} - x_{k,j}\right) \tag{39}$$

where x_i denotes the food supply generated by the employed bees, and n denotes the necessary solution size, random generated number ϕ in the range of 0 and 1, k is a value chosen at random between 0 and the maximum amount of food resources (k≠i), between 0 and the maximum number of solutions, j is a random number (weights).

After all employed bees have completed their search, they waggle dance to communicate the food source information with onlooker bees. An onlooker bee evaluates the nectar data of all used bees and picks a food source which is likely to be proportionate to the quantity of its nectar. This probabilistic selection method is a ''roulette wheel'' selection system, as follows:

$$p_i = \frac{fit_i}{\sum_{j=1}^{SN} fit_j} \tag{40}$$

where, fit_i is the fitness value of the i^{th} swarm solution. It is observed that, the better solution i, the higher probability of the i^{th} food source will be chosen.

The scout bee phase is in charge of determining the maximum number of epochs, which indicates the number of times the solution is permitted to degrade. If a position cannot be enhanced after a certain number of cycles (called a limit), the food supply is thereafter discarded. Assume xi is the discarded source, and the scout bee identifies a new food source to replace it as follows:

$$x_{i,j} = lb_j + \text{rand}(0, 1) \times \left(ub_j - lb_j\right) \tag{41}$$

where, rand(0,1) is a random number within the range [0,1] based on a normal distribution and u_b, l_b are upper and lower boundaries of the j^{th} dimension, respectively.

The ABC algorithm's goal is to discover appropriate weights and optimize them in the search environment. To accomplish this goal, several ABC-ANN patterns with varying numbers of bees were created using the suggested 19 neurons in the ANN structure. As a result, the number of bees will be increased until the minimal error is achieved and the test and error research has been completed to identify additional interconnected factors.

As shown in Table 4, the ABC with 60 bees was recognized as the optimal network established on basis of ranking systems i.e. rank one means optimum number of bees. The test results which obtained from the optimum number of bees in

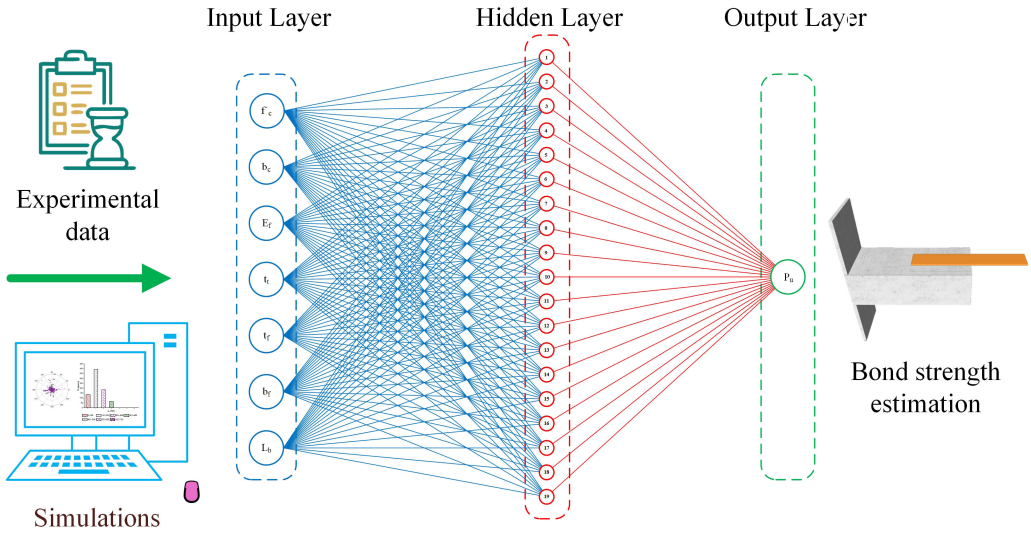

FIGURE 3. Structure of ANN.

TABLE 3. Performance of ANN model.

	Values				Rank				Total
Neurons	R		MSE		R		MSE		
	Training	Testing	Training	Testing	Training	Testing	Training	Testing	
2	0.716473	0.744026	0.010471	0.007833	23	23	23	22	91
3	0.916306	0.900247	0.003199	0.004739	19	17	20	18	74
4	0.914513	0.921919	0.003063	0.003576	20	7	19	7	53
5	0.88878	0.87611	0.003904	0.004254	21	20	21	16	78
6	0.947026	0.909171	0.001996	0.00369	15	15	14	8	52
7	0.939139	0.927144	0.002497	0.002601	17	5	17	2	41
8	0.925985	0.871837	0.002778	0.560747	18	21	18	23	80
9	0.852539	0.876522	0.005873	0.006237	22	19	22	21	84
10	0.954855	0.915595	0.001489	0.004741	10	10	9	19	48
11	0.941753	0.941755	0.002073	0.003436	16	1	15	4	36
12	0.954057	0.913682	0.001673	0.003846	11	12	11	10	44
13	0.950201	0.913521	0.001912	0.003515	12	13	13	5	43
14	0.967068	0.915524	0.001173	0.004157	7	11	6	15	39
15	0.967332	0.928415	0.00127	0.004057	6	4	7	14	31
16	0.947438	0.867898	0.002263	0.004533	14	22	16	17	69
17	0.96961	0.917513	0.001166	0.003946	4	9	4	11	28
18	0.968181	0.928698	0.00117	0.003807	5	3	5	9	22
19	0.97094	0.9378	0.00105	0.00262	3	2	3	3	11
20	0.94822	0.925673	0.00188	0.003975	13	6	12	12	43
21	0.974317	0.87924	0.000885	0.005673	2	18	1	20	41
22	0.974821	0.911626	0.000935	0.004049	1	14	2	13	30
23	0.964004	0.921448	0.001286	0.002384	8	8	8	1	25
24	0.961453	0.904136	0.001551	0.003571	9	16	10	6	41

TABLE 4. Performance of optimized ANN-ABC model.

	Values				Rank				Total
Bee	R		MSE		R		MSE		
	Training	Testing	Training	Testing	Training	Testing	Training	Testing	
30	0.973567	0.942305	0.00102863	0.00233896	1	4	1	4	10
60	0.971409	0.956165	0.00113140	0.00187475	2	1	2	1	6
120	0.965563	0.898635	0.00129347	0.00645214	5	6	5	6	22
300	0.967889	0.944091	0.00124767	0.00254968	4	3	4	5	16
600	0.961630	0.916047	0.00137366	0.00233305	6	5	6	3	20
800	0.969770	0.949751	0.00117621	0.0020747	3	2	3	2	18
1000	0.975795	0.701384	0.00090359	0.0136420	7	7	7	7	28

training and testing 0.971409 and 0.956165 are the R values and significantly tiny values 0.00113140 and 0.00187475 are the normalized MSE values.

C. GAUSSIAN PROCESSED REGRESSION (GPR)

GPR is a Bayesian inference method that works with real-valued variables [102]. It is a non-parametric prediction

TABLE 5. Comparison of ANN, ABC-ANN, and GPR.

Model		R	R^2	RMSE	MSE	MAE
ANN	Training	0.9594	0.9204	2.9221	8.5386	1.7784
	Testing	0.9024	0.8143	3.9301	15.4457	1.7078
	Overall	0.9309	0.8666	3.4760	12.0826	1.7641
ABC-ANN	Training	0.9648	0.9308	2.6576	7.0628	1.7945
	Testing	0.9469	0.8966	2.7045	7.3143	1.7817
	Overall	0.9514	0.9052	2.7254	7.4278	1.7867
GPR	Training	0.9712	0.9432	2.6514	7.0299	1.8012
	Testing	0.9535	0.9092	2.6724	7.1417	1.7994
	Overall	0.9618	0.9251	2.6939	7.2571	1.7985

TABLE 6. Comparison of existing models with developed database.

Method/Model	Statistical Parameters						Standard Deviation
	R	R^2	MSE	RMSE	MAE (kN)	MAPE (%)	
ANN	0.9309	0.8666	12.0826	3.4760	1.7641	11.1545	8.467
ABC-ANN	0.9514	0.9052	7.4278	2.7254	1.7867	9.5196	8.6315
GPR	0.9618	0.9251	7.2571	2.6939	1.7985	7.3413	9.3144
Codal Model-1	0.8619	0.7429	20.1305	4.4867	3.0709	19.2225	7.0867
Codal Model-2	0.8837	0.7809	16.9678	4.1192	2.8763	18.1705	7.7161
Codal Model-3	0.8322	0.6926	23.7481	4.8732	3.3103	20.5316	7.3492
Codal Model-4	0.8063	0.6501	27.0379	5.1998	3.5593	22.3387	7.0747
Codal Model-5	0.8353	0.6977	23.3879	4.8361	3.1909	20.0675	7.3087
Model-1	0.6151	0.3783	87.3664	9.347	4.1518	40.0581	4.4942
Model-2	0.7221	0.5214	57.0040	7.5501	5.0996	27.6575	5.2476
Model-3	0.7213	0.5203	59.3116	7.7014	4.9742	31.1937	8.9441
Model-4	0.7038	0.4953	64.3846	8.024	6.0876	36.3521	9.2735

TABLE 7. Weight and bias of optimized model.

W_i							B_i	W_o	B_o
f'_c	b_c	E_f	f_f	t_f	b_f	L_f			
0.7201	-0.6989	0.2064	0.5074	-0.9519	-1.0143	0.7517	-2.4176	-0.1936	-0.7109
1.0526	-0.8553	0.4387	-0.7200	0.6357	-0.4494	0.3121	-2.3220	0.0519	
0.8038	-0.7584	0.5614	0.0560	-0.6271	-1.0524	-1.5026	-1.5178	0.5274	
1.4747	-0.6307	0.9609	0.3477	-0.9233	-0.5627	-1.0271	-1.0893	-0.7812	
-0.4649	1.1065	0.3478	0.5986	-0.4986	-0.5430	1.6280	1.1316	0.8756	
1.2784	0.3704	1.1721	-1.0203	-1.1734	1.2120	-0.2905	-0.8543	0.5526	
-0.1729	-0.5856	1.2161	-0.8805	0.1060	-1.2538	0.8515	0.8402	0.9406	
-1.1278	-0.0390	-1.2606	-0.8593	-0.4341	1.2062	-0.3233	0.7834	0.2318	
0.3620	-0.1953	-0.9335	0.3031	1.6414	0.3022	-1.8947	0.2403	0.9342	
0.5583	-1.0441	-0.7267	-0.1054	1.2403	0.4098	0.3330	0.9682	0.7306	
0.9561	0.7338	0.9217	1.0387	-1.0626	0.2668	0.1327	0.5890	0.2623	
0.8660	-0.4178	1.1862	0.3691	-0.5312	0.6018	-0.6578	0.5233	0.8498	
1.0431	1.0975	0.5297	1.2053	0.1971	0.6456	-0.4057	0.8172	0.0770	
-0.2575	-0.4735	0.3605	-1.5294	-0.4618	0.4495	0.8015	-1.0374	0.6037	
-0.7865	0.2041	-1.0091	0.0243	0.3639	1.4279	0.1015	-0.5800	0.2161	
-0.5391	-0.1519	-0.7390	0.9679	0.5379	-1.5907	0.7285	-1.8297	-0.4567	
-1.0665	-1.8058	0.6228	-0.0119	-0.7463	0.3329	0.6940	-1.3628	0.4164	
0.0366	1.3431	-0.3301	0.5071	0.8129	-1.4702	-0.6742	1.0882	0.5199	
0.1337	0.5144	0.8085	0.8437	0.7346	0.6395	-0.6729	-2.7585	0.9733	

model for a specific dataset function, D = (x_i, t_i), $i = 1, 2, \ldots, N$ where x_i is an input and t_i is a target variable. A distribution function, termed "Gaussian process regression", which may be expressed as, can be used for the Bayesian regression.

$$P(f \mid D) = \frac{p(f)p(d \mid f)}{p(D)} \tag{42}$$

In GPR a covariance function called k(x, x') is the primary function. Covariance function can be best performed as:

$$k\left(x, x'\right) = \sigma_f^2 \exp\left\{-\frac{1}{2}\left(\frac{x_i - x_j}{l^2}\right)\right\} \tag{43}$$

where, σ_f^2 = maximum permissible variance and l = length of scale. The output of latent function is given as:

$$y = f(x) + \varepsilon \tag{44}$$

where, f(x) = latent function and ε = Gaussian noise. The latent function is treated as a random variable in GPR. If the difference between x and x' approaches zero for the aforementioned covariance function, this indicates that the f(x) function is near to the real function f(x)'. By adding the noise values, the preceding equation may be rewritten as follows.

$$k\left(x, x'\right) = \sigma_f^2 \exp\left\{-\frac{1}{2}\left(\frac{x_i - x_j}{l^2}\right)\right\} + \sigma_n^2 \delta\left(x, x'\right) \tag{45}$$

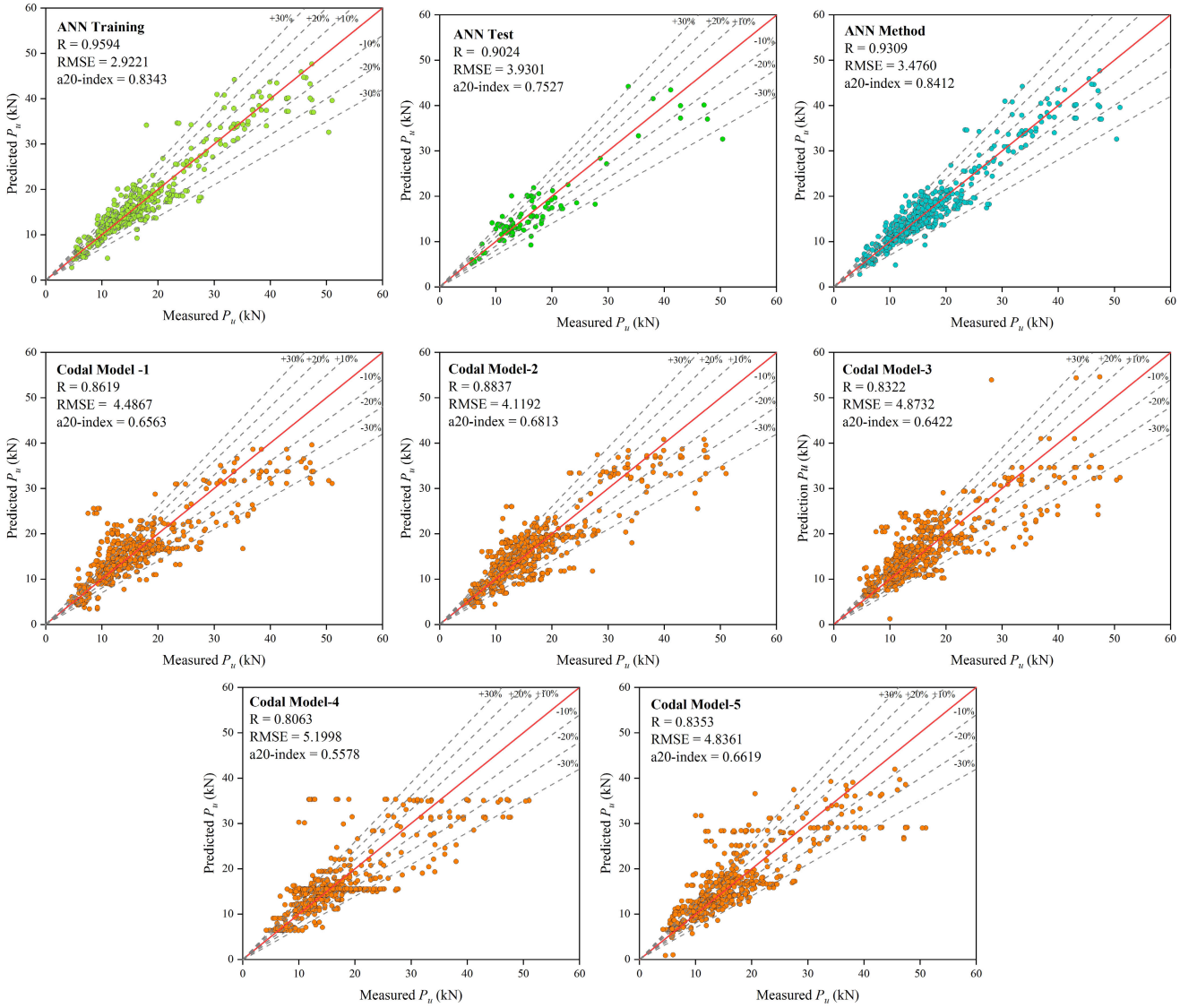

FIGURE 4. Predicted and measured values of ANN Training, ANN Testing, ANN, Codal Model-1, Codal Model-2, Codal Model-3, Codal Model-4 and Codal Model-5.

where, σ_n^2 = variance of n observations and δ(x, x') = Kronecker delta function. The prediction function can be written as:

$$y = f(x) + N\left(0, \sigma_n^2\right) \tag{46}$$

The kernel or covariance function k(x, x') given as:

$$K = \begin{bmatrix} k(x_1, x_2) & k(x_1, x_2) & \dots & k(x_1, x_n) \\ k(x_2, x_1) & k(x_2, x_2) & \dots & k(x_2, x_n) \\ \vdots & \vdots & & \vdots \\ k(x_n, x_1) & k(x_n, x_2) & \dots & k(x_n, x_n) \end{bmatrix} \tag{47}$$

V. COMPARISON OF PERFORMANCE OF AI MODELS AND EXISTING MODEL

The ANN, mutated ABC-ANN and GPR model, testing and training outcomes are assessed using equations 33 to 38, used to find out the performance and errors in the predicted values. It should be highlighted that these criteria are evaluated using actual targets created by standardized data in order to offer a clear comparison of model error values. The detailed of each analyzed model is tabulated in Table 5.

The ANN, mutated ABC-ANN, and GPR results are compared to the earlier work, methodologies, and international codes which are mentioned in equation 1 to equation 30. Table 6 illustrates the findings of test results obtained from

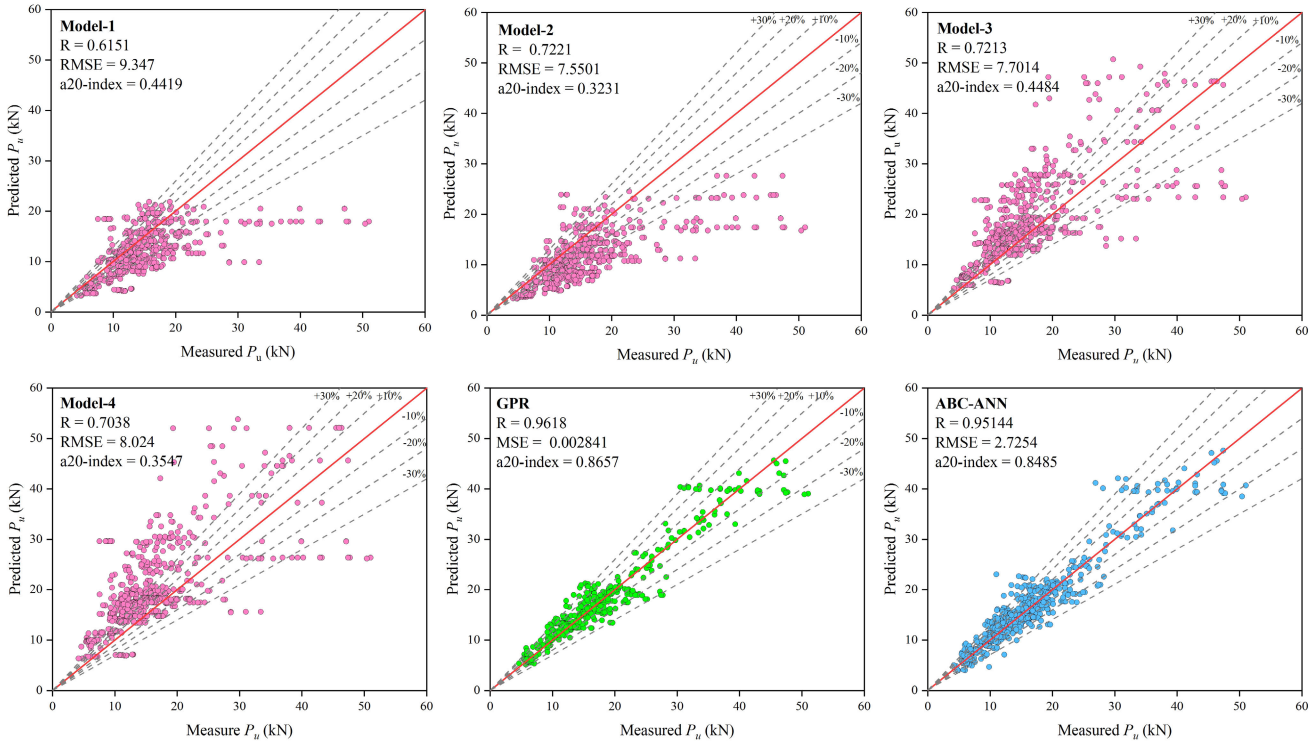

FIGURE 5. Predicted and measured values of Model-1, Model-2, Model-3, Model-4, GPR and ABC-ANN.

statistical criteria, coefficient of determination R-squared (R^2), correlation coefficient (R), as well as error markers of RMSE, MSE, MAE and MAPE. The standard deviation of the original data is 8.7965 which is quite closer to the ABC-ANN model data.

Figure 4 and Figure 5 depicts the comparsion study of experimental measured with respect to the predicted data using various AI algorithms and existing models.

Figure 6 depicts the scattering of absolute error values (AEV) (kN), so that the error value of the recommended approaches may be compared directly with those of the existing literature models and codal standards. The spreading of values in mutated ANN and GPR models are more focused within the 5 kN range of bond strength. As a consequence, the ABC-ANN and GPR model may be concluded that they are superior than other approaches and have the best precision and robustness. As a result, the AEV of ABC-ANN and GPR are almost (approximately 94.37% of the time) less than 5.98 kN and (approximately 94.33% of the time) less than 5.98 kN respectively.

VI. PROPOSED FORMULATION FROM ABC-ANN

The operation of ANN is only feasible, when the network's input and output weights, as well as bias values, are known at multiple levels. The predicted FRP-concrete bond strength may be calculated using excel spreadsheet application utilizing the findings presented in this Table 7 as a direct form of prediction formulation. Table 7 shows the weight and bias

TABLE 8. List of Symbols.

Symbol	Description
f'_c	Compressive strength of concrete (MPa)
b_f	Width of the FRP laminate/fabric (mm)
E_f	Modulus of elasticity of FRP material (GPa)
t_f	Thickness of FRP material (mm)
b_c	Width of concrete block (mm)
f_f	Tensile strength of FRP composite (MPa)
L_b	Length FRP bonded material (mm)
k_p	Geometric factor
L_e	Effective length (mm)
P_u	Applied load (kN)
β_p and β_L	Geometric parameters
k_f	Specific fracture energy
d_f	Thickness of the failure plane
τ_f	Peak interface shear stress
δ_f	Slip at maximum interface shear stress
f_{ct}	Characteristic axial tensile strength of concrete (MPa)
f_c	Mean value of concrete tensile strength (MPa)

used for predicting the output values. These values are used to find out the X_1 to X_{19} constants which were used in the equation 48.

$$X_i = \tanh\left(W_i X_{i,n\ orm} + B_i\right) \quad (48)$$

$$P_{upredicted} = \text{purlin}\left(W_o X_i + B_o\right) = W_o X_i + B_o \quad (49)$$

Table 7 shows the values which contains different parameters to evaluate the bond strength with other constant values and having activation function 'tansig'. Equation 49 might

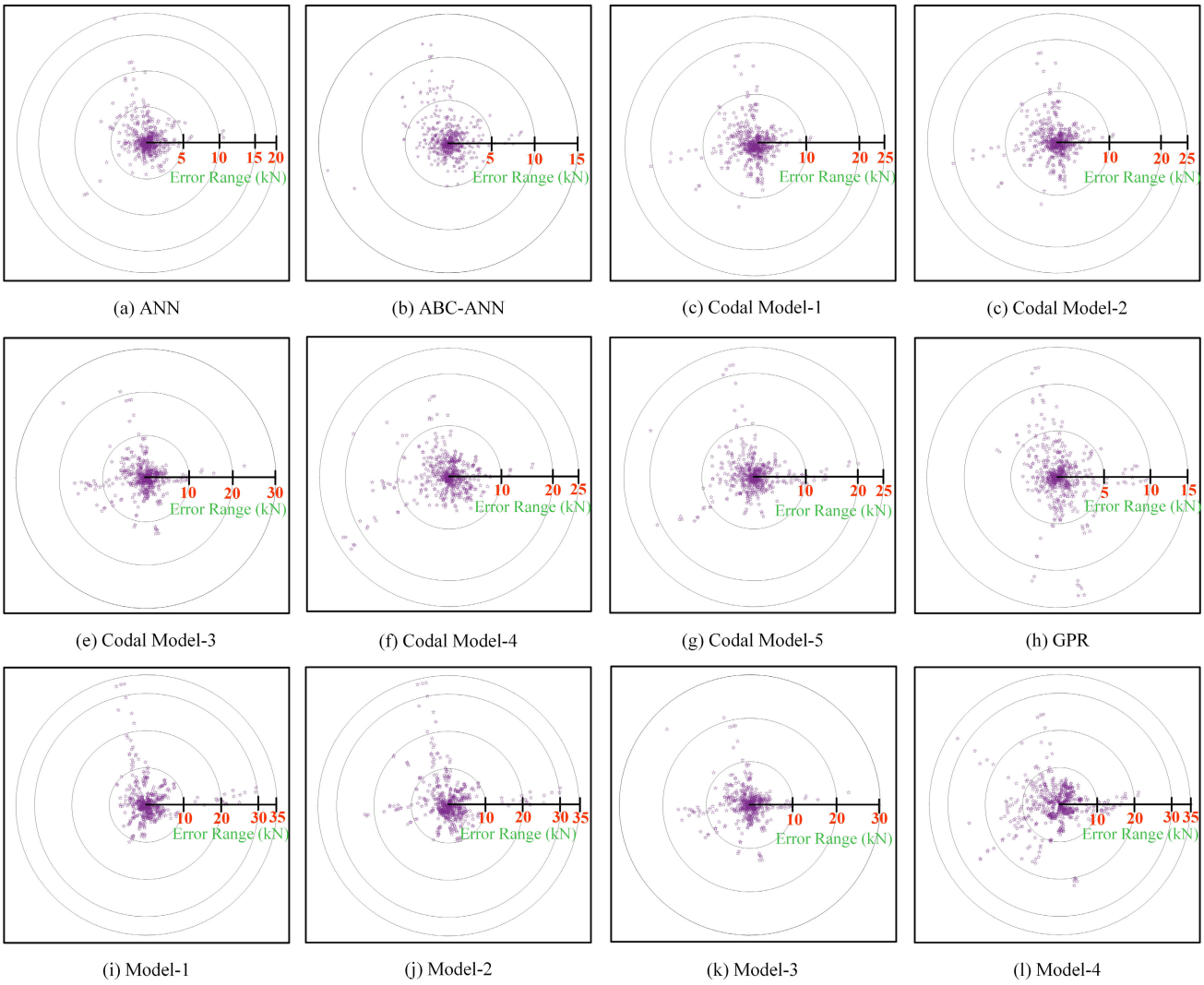

FIGURE 6. Absolute error values.

predict bond strength with up to 94 percent accuracy. Put all the measured values form above mentioned equation in equation 49.

VII. CONCLUSION AND FUTURE SCOPE

In this article, the FRP-concrete bond strength is evaluated using an ANN, ABC-ANN, and GPR techniques. A hybrid method ABC-ANN is used to optimize the ANN model for better bond strength predictions. In this case, 744 experimental data were gathered from the literature, including concrete compressive strength, FRP laminate/fabric width, FRP material modulus of elasticity, FRP material thickness, concrete block width, FRP composite tensile strength, and FRP bonded material length. All of the data utilized was scaled and standardized between 0 and 1 in order to get the appropriate responses. The ANN, ABC-ANN, and GPR prediction findings were compared with current techniques for evaluating the bond strength of FRP-concrete given by international codal standards and the other four models from the prior literature study. In ANN and ABC-ANN, 70% of the data is utilized for training, 15% for testing, and the remaining 15% for validation. The accuracy of bond strength estimate might be improved by using these two methods, ABC-ANN and GPR. The empirically suggested formulation, which was built utilizing the mutated ABC with ANN's weights and bias, may be easily implemented for bond strength evaluation. The ABC-ANN and GPR prediction results are accurate for more than 90% of experimental data. The main limitations of this work is that a user can only use the proposed model of this article for an input vector that be within the interval of each input variable. Researchers and FRP applicators may benefit from using this model, because it provides good accuracy and consume less time. This model may be used by FRP applicators and FRP manufacturing companies to enhance the bonding capacity of existing adhesives and FRP systems. In future research, the accuracy of this model might

be improved by employing a larger number of experimental databases and comparing it to all natural-inspired algorithms in order to improve the prediction of FRP concrete bond strength.

REFERENCES

[1] R. Kumar and P. Gardoni, "Stochastic modeling of deterioration in buildings and civil infrastructure," in *Handbook of Seismic Risk Analysis and Management of Civil Infrastructure Systems*, S. Tesfamariam and K. Goda, Eds. Sawston, U.K.: Woodhead Publishing, 2013, ch. 16, pp. 410–434.

[2] A. James, E. Bazarchi, A. A. Chiniforush, P. P. Aghdam, M. R. Hosseini, A. Akbarnezhad, I. Martek, and F. Ghodoosi, "Rebar corrosion detection, protection, and rehabilitation of reinforced concrete structures in coastal environments: A review," *Construct. Building Mater.*, vol. 224, pp. 1026–1039, Nov. 2019, doi: 10.1016/j.conbuildmat.2019.07.250.

[3] R. D. Borcherdt, R. O. Hamburger, and C. A. Kircher, "Seismic design provisions and guidelines in the United States: A prologue," in *International Geophysics*, vol. 81, W. H. K. Lee, H. Kanamori, P. C. Jennings, and C. Kisslinger, Eds. New York, NY, USA: Academic, 2003, ch. 68, pp. 1127–1132.

[4] M. U. Khan, S. Ahmad, and H. J. Al-Gahtani, "Chloride-induced corrosion of steel in concrete: An overview on chloride diffusion and prediction of corrosion initiation time," *Int. J. Corrosion*, vol. 2017, Feb. 2017, Art. no. 5819202, doi: 10.1155/2017/5819202.

[5] J. A. Mullard and M. G. Stewart, "Life-cycle cost assessment of maintenance strategies for RC structures in chloride environments," *J. Bridge Eng.*, vol. 17, no. 2, pp. 353–362, 2012, doi: 10.1061/(ASCE)BE.1943-5592.0000248.

[6] I. Navarro, V. Yepes, and J. Martí, "Life cycle cost assessment of preventive strategies applied to prestressed concrete bridges exposed to chlorides," *Sustainability*, vol. 10, no. 3, p. 845, Mar. 2018, doi: 10.3390/su10030845.

[7] E. Chen, C. G. Berrocal, I. Löfgren, and K. Lundgren, "Correlation between concrete cracks and corrosion characteristics of steel reinforcement in pre-cracked plain and fibre-reinforced concrete beams," *Mater. Struct.*, vol. 53, no. 2, p. 33, Apr. 2020, doi: 10.1617/s11527-020-01466-z.

[8] S. Robuschi, A. Tengattini, J. Dijkstra, I. Fernandez, and K. Lundgren, "A closer look at corrosion of steel reinforcement bars in concrete using 3D neutron and X-ray computed tomography," *Cement Concrete Res.*, vol. 144, Jun. 2021, Art. no. 106439, doi: 10.1016/j.cemconres.2021.106439.

[9] J.-S. Jung, B. Y. Lee, and K.-S. Lee, "Experimental study on the structural performance degradation of corrosion-damaged reinforced concrete beams," *Adv. Civil Eng.*, vol. 2019, Oct. 2019, Art. no. 9562574, doi: 10.1155/2019/9562574.

[10] I. Fernandez, M. F. Herrador, A. R. Marí, and J. M. Bairán, "Ultimate capacity of corroded statically indeterminate reinforced concrete members," *Int. J. Concrete Struct. Mater.*, vol. 12, no. 1, p. 75, Dec. 2018, doi: 10.1186/s40069-018-0297-9.

[11] K. Darain, M. Jumaat, A. Shukri, M. Obaydullah, M. Huda, M. Hosen, and N. Hoque, "Strengthening of RC beams using externally bonded reinforcement combined with near-surface mounted technique," *Polymers*, vol. 8, no. 7, p. 261, Jul. 2016, doi: 10.3390/polym8070261.

[12] M. Akiyama, D. M. Frangopol, and K. Takenaka, "Reliability-based durability design and service life assessment of reinforced concrete deck slab of jetty structures," *Struct. Infrastruct. Eng.*, vol. 13, no. 4, pp. 468–477, Apr. 2017, doi: 10.1080/15732479.2016.1164725.

[13] F. Jiang, X. Wan, F. H. Wittmann, and T. Zhao, "Influence of combined actions on durability of reinforced concrete structures," *Restoration Buildings Monuments*, vol. 17, no. 5, pp. 289–298, Oct. 2011, doi: 10.1515/rbm-2011-6466.

[14] A. Bossio, F. Fabbrocino, T. Monetta, G. P. Lignola, A. Prota, G. Manfredi, and F. Bellucci, "Corrosion effects on seismic capacity of reinforced concrete structures," *Corrosion Rev.*, vol. 37, no. 1, pp. 45–56, Jan. 2019, doi: 10.1515/corrrev-2018-0044.

[15] Y. Zhou, B. Gencturk, K. Willam, and A. Attar, "Carbonation-induced and chloride-induced corrosion in reinforced concrete structures," *J. Mater. Civil Eng.*, vol. 27, no. 9, 2015, Art. no. 04014245, doi: 10.1061/(ASCE)MT.1943-5533.0001209.

[16] R. E. Melchers, "Modelling durability of reinforced concrete structures," *Corrosion Eng., Sci. Technol.*, vol. 55, no. 2, pp. 171–181, Feb. 2020, doi: 10.1080/1478422X.2019.1710660.

[17] U. Meier, M. Deuring, H. Meier, and G. Schwegler, "CFRP bonded sheets," in *Fiber-Reinforced-Plastic (FRP) Reinforcement for Concrete Structures*, A. Nanni, Ed. Oxford, U.K.: Elsevier, 1993, pp. 423–434, doi: 10.1016/B978-0-444-89689-6.50023-9.

[18] Y. Kanaori and S.-I. Kawakami, "The 1995 7.2 magnitude Kobe earthquake and the Arima-Takatsuki tectonic line: Implications of the seismic risk for central Japan," *Eng. Geol.*, vol. 43, nos. 2–3, pp. 135–150, 1996, doi: 10.1016/0013-7952(96)00056-7.

[19] H. Fukuyama, G. Tumialan, and A. Nanni, "Japanese design and construction guidelines for seismic retrofit of building structures with FRP composites," presented at the 2nd Int. Conf. FRP Compos. Civil Eng. Hong Kong Inst. Eng., Hong Kong, 2001.

[20] U. M. Angst, "Challenges and opportunities in corrosion of steel in concrete," *Mater. Struct.*, vol. 51, no. 1, pp. 1–20, Feb. 2018, doi: 10.1617/s11527-017-1131-6.

[21] D. Rajak, D. Pagar, P. Menezes, and E. Linul, "Fiber-reinforced polymer composites: Manufacturing, properties, and applications," *Polymers*, vol. 11, no. 10, p. 1667, Oct. 2019, doi: 10.3390/polym11101667.

[22] N. L. Feng, S. D. Malingam, and S. Irulappasamy, "Bolted joint behavior of hybrid composites," in *Failure Analysis in Biocomposites, Fibre-Reinforced Composites and Hybrid Composites*, M. Jawaid, M. Thariq, and N. Saba, Eds. Sawston,U.K.: Woodhead Publishing, 2019, ch. 4, pp. 79–95, doi: 10.1016/B978-0-08-102293-1.00004-8.

[23] N. Chand and M. Fahim, "Introduction to tribology of polymer composites," in *Tribology of Natural Fiber Polymer Composites,* N. Chand and M. Fahim, Eds. Sawston, U.K.: Woodhead Publishing, 2008, ch. 2, pp. 59–83, doi: 10.1533/9781845695057.59.

[24] M. A. Masuelli, "Introduction of fibre-reinforced polymers- polymers and composites: Concepts, properties and processes," in *Fiber Reinforced Polymers-the Technology Applied for Concrete Repair*, N. Chand and M. Fahim, Eds. Sawston, U.K.: Woodhead Publishing, 2013, doi: 10.5772/54629.

[25] F. Campbell, *Structural Composite Materials*. The Netherlands: ASM Digital Library, 2010, doi: 10.31399/asm.tb.scm.9781627083140.

[26] P. W. R. Beaumont, "The structural integrity of composite materials and long-life implementation of composite structures," *Appl. Compos. Mater.*, vol. 27, no. 5, pp. 449–478, Oct. 2020, doi: 10.1007/s10443-020-09822-6.

[27] A. Godat, F. Hammad, and O. Chaallal, "State-of-the-art review of anchored FRP shear-strengthened RC beams: A study of influencing factors," *Compos. Struct.*, vol. 254, Dec. 2020, Art. no. 112767, doi: 10.1016/j.compstruct.2020.112767.

[28] L. S. Lee and R. Jain, "The role of FRP composites in a sustainable world," *Clean Technol. Environ. Policy*, vol. 11, no. 3, pp. 247–249, Sep. 2009, doi: 10.1007/s10098-009-0253-0.

[29] A. Hosseini and D. Mostofinejad, "Effective bond length of FRP-to-concrete adhesively-bonded joints: Experimental evaluation of existing models," *Int. J. Adhes. Adhesives*, vol. 48, pp. 150–158, Jan. 2014, doi: 10.1016/j.ijadhadh.2013.09.022.

[30] H. Jahangir and M. R. Esfahani, "Numerical study of bond–slip mechanism in advanced externally bonded strengthening composites," *KSCE J. Civil Eng.*, vol. 22, no. 11, pp. 4509–4518, 2018, doi: 10.1007/s12205-018-1662-6.

[31] C. Mensah, Z. Wang, A. O. Bonsu, and W. Liang, "Effect of different bond parameters on the mechanical properties of FRP and concrete interface," *Polymers*, vol. 12, no. 11, p. 2466, Oct. 2020, doi: 10.3390/polym12112466.

[32] "Externally bonded FRP reinforcement for RC structures," Eur. Union, fib Bulletin no. 14, 2001.

[33] *Guide for the Design and Construction of Externally Bonded FRP Systems for Strengthening Existing structures*, Rome, Italy, 2004.

[34] *Guide for the Design and Construction of Externally Bonded FRP Systems for Strengthening Concrete Structures*, Standard ACI440.2R.08, 2008.

[35] *Design Handbook for RC Structures Retrofitted With FRP and Metal Plates: Beams and Slabs*, Standards Australia Sydney, Sydney, NSW, Australia, 2008.

[36] *Design Guidance for Strengthening Concrete Structures Using Fibre Composites Materials Concrete Society*, document CS-TR-55-U.K., 2013.

[37] P. Sarir, J. Chen, P. G. Asteris, D. J. Armaghani, and M. M. Tahir, "Developing GEP tree-based, neuro-swarm, and whale optimization models for evaluation of bearing capacity of concrete-filled steel tube columns," *Eng. with Comput.*, vol. 37, no. 1, pp. 1–19, Jan. 2021, doi: 10.1007/s00366-019-00808-y.

[38] M. Y. Mansour, M. Dicleli, J. Y. Lee, and J. Zhang, "Predicting the shear strength of reinforced concrete beams using artificial neural networks," *Eng. Struct.*, vol. 26, no. 6, pp. 781–799, May 2004, doi: 10.1016/j.engstruct.2004.01.011.

[39] M. Apostolopoulou, P. G. Asteris, D. J. Armaghani, M. G. Douvika, P. B. Lourenço, L. Cavaleri, A. Bakolas, and A. Moropoulou, "Mapping and holistic design of natural hydraulic lime mortars," *Cement Concrete Res.*, vol. 136, Oct. 2020, Art. no. 106167, doi: 10.1016/j.cemconres.2020.106167.

[40] L. Sun, M. Koopialipoor, D. Jahed Armaghani, R. Tarinejad, and M. M. Tahir, "Applying a meta-heuristic algorithm to predict and optimize compressive strength of concrete samples," *Eng. Comput.*, vol. 37, no. 2, pp. 1133–1145, Apr. 2021, doi: 10.1007/s00366-019-00875-1.

[41] J. Gao, M. Koopialipoor, D. J. Armaghani, A. Ghabussi, S. Baharom, A. Morasaei, A. Shariati, M. Khorami, and J. Zhou, "Evaluating the bond strength of FRP in concrete samples using machine learning methods," *Smart Struct. Syst.*, vol. 26, no. 4, pp. 403–418, 2020, doi: 10.12989/sss.2020.26.4.403.

[42] M. Khorshidi Paji, B. Gordan, M. Biklaryan, D. J. Armaghani, J. Zhou, and M. Jamshidi, "Neuro-swarm and neuro-imperialism techniques to investigate the compressive strength of concrete constructed by freshwater and magnetic salty water," *Measurement*, vol. 182, Sep. 2021, Art. no. 109720, doi: 10.1016/j.measurement.2021.109720.

[43] A. Dehghanbanadaki, M. Khari, S. T. Amiri, and D. J. Armaghani, "Estimation of ultimate bearing capacity of driven piles in c-φ soil using MLP-GWO and ANFIS-GWO models: A comparative study," *Soft Comput.*, vol. 25, no. 5, pp. 4103–4119, 2021, doi: 10.1007/s00500-020-05435-0.

[44] M. Khari, D. Jahed Armaghani, and A. Dehghanbanadaki, "Prediction of lateral deflection of small-scale piles using hybrid PSO–ANN model," *Arabian J. Sci. Eng.*, vol. 45, no. 5, pp. 3499–3509, 2020, doi: 10.1007/s13369-019-04134-9.

[45] P. G. Asteris, D. J. Armaghani, G. D. Hatzigeorgiou, C. G. Karayannis, and K. Pilakoutas, "Predicting the shear strength of reinforced concrete beams using artificial neural networks," *Comput. Concrete*, vol. 24, no. 5, pp. 469–488, 2019, doi: 10.12989/cac.2019.24.5.469.

[46] E. Momeni, A. Yarivand, M. B. Dowlatshahi, and D. J. Armaghani, "An efficient optimal neural network based on gravitational search algorithm in predicting the deformation of geogrid-reinforced soil structures," *Transp. Geotechnics*, vol. 26, Jan. 2021, Art. no. 100446, doi: 10.1016/j.trgeo.2020.100446.

[47] J. Liao, P. G. Asteris, L. Cavaleri, A. S. Mohammed, M. E. Lemonis, M. Z. Tsoukalas, A. D. Skentou, C. Maraveas, M. Koopialipoor, and D. J. Armaghani, "Novel fuzzy-based optimization approaches for the prediction of ultimate axial load of circular concrete-filled steel tubes," *Buildings*, vol. 11, no. 12, p. 629, Dec. 2021, doi: 10.3390/buildings11120629.

[48] A. Mohammed, R. Kurda, D. J. Armaghani, and M. Hasanipanah, "Prediction of compressive strength of concrete modified with fly ash: Applications of neuro-swarm and neuro-imperialism models," *Comput. Concrete*, vol. 27, no. 5, pp. 451–489, 2021, doi: 10.12989/cac.2021.27.5.489.

[49] D. C. Feng, B. Cetiner, M. R. A. Kakavand, and E. Taciroglu, "Data-driven approach to predict the plastic Hinge length of reinforced concrete columns and its application," *J. Struct. Eng.*, vol. 147, no. 2, 2021, Art. no. 04020332, doi: 10.1061/(ASCE)ST.1943-541X.0002852.

[50] M. J. Chajes, W. Finch, and T. A. Thomson, "Bond and force transfer of composite-material plates bonded to concrete," *Struct. J.*, vol. 93, no. 2, pp. 209–217, 1996.

[51] T. Maeda, "A study on bond mechanism of carbon fiber sheet," in *Proc. FRPTCS*, vol. 1, 1997, pp. 279–286.

[52] B. Täljsten, "Defining anchor lengths of steel and CFRP plates bonded to concrete," *Int. J. Adhes. Adhesives*, vol. 17, no. 4, pp. 319–327, Nov. 1997.

[53] T. Ueda, Y. Sato, and Y. Asano, "Experimental study on bond strength of continuous carbon fiber sheet," *Special Publication*, vol. 188, pp. 407–416, Aug. 1999.

[54] H. Zhao, Y. Zhang, and M. Zhao, "Research on the bond performance between CFRP plate and concrete," in *Proc. 1st Conf. FRP Concrete Struct. China*, 2000, pp. 247–253.

[55] Z. Wu, H. Yuan, H. Yoshizawa, and T. Kanakubo, "Experimental/analytical study on interfacial fracture energy and fracture propagation along FRP-concrete i nterface," *Special Publication*, vol. 201, pp. 133–152, Jul. 2001.

[56] B. B. Adhikary and H. Mutsuyoshi, "Study on the bond between concrete and externally bonded CFRP sheet," in *Proc. 5th Int. Conf. Fibre-Reinforced Plastics Reinforced Concrete Struct.* Cambridge, U.K.: Thomas Telford Publishing, 2001, pp. 371–378.

[57] F.-Q. Xu, J. Guan, and Y. Chen, "Bond strength between C-FRP sheets and concrete," in *Proc. 1st Conf. FRP Compos. Civil Eng.*, Hong Kong, vol. 1, 2001, pp. 357–364.

[58] K. Nakaba, T. Kanakubo, T. Furuta, and H. Yoshizawa, "Bond behavior between fiber-reinforced polymer laminates and concrete," *Struct. J.*, vol. 98, no. 3, pp. 359–367, 2001.

[59] Z. Tan, "Experimental research for RC beam strengthened with GFRP," M.S. thesis, Dept. Civil Eng., Tsinghua Univ., Beijing, China, 2002.

[60] J.-G. Dai, Y. Sato, and T. Ueda, "Improving the load transfer and effective bond length for FRP composites bonded to concrete," *Jpn. Concrete Inst.*, vol. 24, no. 2, pp. 1423–1428, 2002.

[61] H. T. Ren, "Study on basic theories and longtime behavior of concrete structures strengthened by fiber reinforced polymers," Ph.D. dissertation, Dept. Civil Eng., Dalian Univ. Technol., Liaoning, China, 2003.

[62] J. Yao, J. G. Teng, and J. F. Chen, "Experimental study on FRP-to-concrete bonded joints," *Compos. B, Eng.*, vol. 36, no. 2, pp. 99–113, Mar. 2005, doi: 10.1016/j.compositesb.2004.06.001.

[63] J. Dai, T. Ueda, and Y. Sato, "Development of the nonlinear bond stress–slip model of fiber reinforced plastics sheet–concrete interfaces with a simple method," *J. Compos. Construct.*, vol. 9, no. 1, pp. 52–62, 2005, doi: 10.1061/(ASCE)1090-0268(2005)9:1(52).

[64] S. K. Sharma, M. S. Mohamed Ali, D. Goldar, and P. K. Sikdar, "Plate–concrete interfacial bond strength of FRP and metallic plated concrete specimens," *Compos. B, Eng.*, vol. 37, no. 1, pp. 54–63, 2006, doi: 10.1016/j.compositesb.2005.05.011.

[65] H. Toutanji, P. Saxena, L. Zhao, and T. Ooi, "Prediction of interfacial bond failure of FRP–concrete surface," *J. Compos. Construct.*, vol. 11, no. 4, pp. 427–436, 2007. [Online]. Available: https://doi.org/10.1061/(ASCE)1090-0268(2007)11:4(427)

[66] Y. Yun and Y.-F. Wu, "Durability of CFRP–concrete joints under freeze–thaw cycling," *Cold Regions Sci. Technol.*, vol. 65, no. 3, pp. 401–412, 2011, doi: 10.1016/j.coldregions.2010.11.008.

[67] F. Ceroni, A. Garofano, and M. Pecce, "Modelling of the bond behaviour of tuff elements externally bonded with FRP sheets," *Compos. B, Eng.*, vol. 59, pp. 248–259, Mar. 2014, doi: 10.1016/j.compositesb.2013.12.007.

[68] W. Li, J. Li, X. Ren, C. K. Y. Leung, and F. Xing, "Coupling effect of concrete strength and bonding length on bond behaviors of fiber reinforced polymer–concrete interface," *J. Reinforced Plastics Compos.*, vol. 34, no. 5, pp. 421–432, 2015, doi: 10.1177/0731684415573816.

[69] S. Ueno, H. Toutanji, and R. Vuddandam, "Introduction of a stress state criterion to predict bond strength between FRP and concrete substrate," *J. Compos. Construct.*, vol. 19, no. 1, 2015, Art. no. 04014024, doi: 10.1061/(ASCE)CC.1943-5614.0000481.

[70] C. Chen, X. Li, D. Zhao, Z. Huang, L. Sui, F. Xing, and Y. Zhou, "Mechanism of surface preparation on FRP-concrete bond performance: A quantitative study," *Compos. B,Eng.*, vol. 163, pp. 193–206, Apr. 2019, doi: 10.1016/j.compositesb.2018.11.027.

[71] C. Yuan, W. Chen, T. M. Pham, and H. Hao, "Effect of aggregate size on bond behaviour between basalt fibre reinforced polymer sheets and concrete," *Compos. B, Eng.*, vol. 158, pp. 459–474, Feb. 2019, doi: 10.1016/j.compositesb.2018.09.089.

[72] D. Mostofinejad, K. Sanginabadi, and M. R. Eftekhar, "Effects of coarse aggregate volume on CFRP-concrete bond strength and behavior," *Construct. Building Mater.*, vol. 198, pp. 42–57, Feb. 2019, doi: 10.1016/j.conbuildmat.2018.11.188.

[73] M. Heydari Mofrad, D. Mostofinejad, and A. Hosseini, "A generic nonlinear bond-slip model for CFRP composites bonded to concrete substrate using EBR and EBROG techniques," *Compos. Struct.*, vol. 220, pp. 31–44, Jul. 2019, doi: 10.1016/j.compstruct.2019.03.063.

[74] P. Zhang, D. Lei, Q. Ren, J. He, H. Shen, and Z. Yang, "Experimental and numerical investigation of debonding process of the FRP plate-concrete interface," *Construct. Building Mater.*, vol. 235, Feb. 2020, Art. no. 117457, doi: 10.1016/j.conbuildmat.2019.117457.

[75] C. Yuan, W. Chen, T. M. Pham, H. Hao, J. Cui, and Y. Shi, "Interfacial bond behaviour between hybrid carbon/basalt fibre composites and concrete under dynamic loading," *Int. J. Adhes. Adhesives*, vol. 99, Jun. 2020, Art. no. 102569, doi: 10.1016/j.ijadhadh.2020.102569.
[76] A. Moghaddas, D. Mostofinejad, A. Saljoughian, and E. Ilia, "An empirical FRP-concrete bond-slip model for externally-bonded reinforcement on grooves," *Construct. Building Mater.*, vol. 281, Apr. 2021, Art. no. 122575, doi: 10.1016/j.conbuildmat.2021.122575.
[77] U. Neubauer and F. Rostasy, "Design aspects of concrete structures strengthened with externally bonded CFRP-plates," presented at the 7th Int. Conf. Struct. Faults and Repair, 1997.
[78] J. F. Chen and J. G. Teng, "Anchorage strength models for FRP and steel plates bonded to concrete," *J. Struct. Eng.*, vol. 127, no. 7, pp. 784–791, 2001, doi: 10.1061/(ASCE)0733-9445(2001)127:7(784).
[79] R. Seracino, M. R. Raizal Saifulnaz, and D. J. Oehlers, "Generic debonding resistance of EB and NSM plate-to-concrete joints," *J. Compos. Construct.*, vol. 11, no. 1, pp. 62–70, 2007, doi: 10.1061/(ASCE)1090-0268(2007)11:1(62).
[80] Y. Pan, G. Xian, and M. A. G. Silva, "Effects of water immersion on the bond behavior between CFRP plates and concrete substrate," *Construct. Building Mater.*, vol. 101, pp. 326–337, Dec. 2015, doi: 10.1016/j.conbuildmat.2015.10.129.
[81] *International Symposium on Latest Achievement of Technology and Research on Retrofitting Concrete Structures*, Japan Concrete Inst., Kyoto, Japan, 2003.
[82] A. Khalifa, J. Gold William, A. Nanni, and M. I. A. Aziz, "Contribution of externally bonded FRP to shear capacity of RC flexural members," *J. Compos. Construct.*, vol. 2, no. 4, pp. 195–202, 1998, doi: 10.1061/(ASCE)1090-0268(1998)2:4(195).
[83] T. Kanakubo, "Third international symposium on non-metallic (FRP) reinforcement for concrete structures (FRPRCS-3)," *Mater. Struct.*, vol. 31, no. 4, pp. 285–287, 1999, doi: 10.1007/BF02480431.
[84] D.-S. Yang, S.-N. Hong, and S.-K. Park, "Experimental observation on bond-slip behavior between concrete and CFRP plate," *Int. J. Concrete Struct. Mater.*, vol. 1, no. 1, pp. 37–43, 2007, doi: 10.4334/IJCSM.2007.1.1.037.
[85] D. Fózer, A. J. Tóth, P. S. Varbanov, J. J. Klemeš, and P. Mizsey, "Sustainability assessment of biomethanol production via hydrothermal gasification supported by artificial neural network," *J. Cleaner Prod.*, vol. 318, Oct. 2021, Art. no. 128606, doi: 10.1016/j.jclepro.2021.128606.
[86] H. Wu, Y. Zhou, Q. Luo, and M. A. Basset, "Training feedforward neural networks using symbiotic organisms search algorithm," *Comput. Intell. Neurosci.*, vol. 2016, pp. 1–14, 2016, doi: 10.1155/2016/9063065.
[87] V. Giurgiutiu, "Signal processing and pattern recognition for structural health monitoring with PWAS transducers," in *Structural Health Monitoring With Piezoelectric Wafer Active Sensors*, 2nd ed., V. Giurgiutiu, Ed. Oxford,U.K.: Academic, 2014, ch. 14, pp. 807–862, doi: 10.1016/B978-0-12-418691-0.00014-9.
[88] H. Alemu, W. Wu, and J. Zhao, "Feedforward neural networks with a hidden layer regularization method," *Symmetry*, vol. 10, no. 10, p. 525, Oct. 2018, doi: 10.3390/sym10100525.
[89] S. Sieniutycz, "Complex systems of neural networks," in *Complexity and Complex Thermo-Economic Systems*, S. Sieniutycz, Ed. Amsterdam, The Netherlands: Elsevier, 2020, Ch. 4, pp. 51–84, doi: 10.1016/B978-0-12-818594-0.00004-0.
[90] S.-I. Lee, S.-H. Shin, and B. Hwang, "Application of artificial neural network to the prediction of tensile properties in high-strength low-carbon bainitic steels," *Metals*, vol. 11, no. 8, p. 1314, Aug. 2021, doi: 10.3390/met11081314.
[91] M. A. Mohammed, M. S. Ahmad, and S. A. Mostafa, "Using genetic algorithm in implementing capacitated vehicle routing problem," in *Proc. Int. Conf. Comput. Inf. Sci. (ICCIS)*, vol. 1, Jun. 2012, pp. 257–262.
[92] S. A. Mostafa, M. S. Ahmad, A. Mustapha, and M. A. Mohammed, "Formulating layered adjustable autonomy for unmanned aerial vehicles," *Int. J. Intell. Comput. Cybern.*, vol. 10, no. 4, pp. 430–450, Nov. 2017, doi: 10.1108/IJICC-02-2017-0013.
[93] S. A. Mostafa, S. S. Gunasekaran, A. Mustapha, M. A. Mohammed, and W. M. Abduallah, "Modelling an adjustable autonomous multi-agent Internet of Things system for elderly smart home," in *Proc. Int. Conf. Appl. Hum. Factors Ergonom.* Cham, Switzerland: Springer, 2019, pp. 301–311.
[94] M. K. A. Ghani, M. A. Mohammed, M. S. Ibrahim, S. A. Mostafa, and D. A. Ibrahim, "Implementing an efficient expert system for services center management by fuzzy logic controller," *J. Theor. Appl. Inf. Technol.*, vol. 95, no. 13, pp. 3127–3135, 2017.
[95] M. Abed Mohammed, B. Al-Khateeb, and D. Ahmed Ibrahim, "Case based reasoning shell frameworkas decision support tool," *Indian J. Sci. Technol.*, vol. 9, no. 42, pp. 1–8, Nov. 2016.
[96] (2021). *A MATLAB Simulink–Mathworks*. [Online]. Available: https://in.mathworks.com/products/MATLAB.html
[97] B. Gordan, D. J. Armaghani, M. Hajihassani, and M. Monjezi, "Prediction of seismic slope stability through combination of particle swarm optimization and neural network," *Eng. Comput.*, vol. 32, no. 1, pp. 85–97, 2016, doi: 10.1007/s00366-015-0400-7.
[98] K.-H. Chang, "Design optimization," in *e-Design*, K.-H. Chang, Ed. Boston, MA, USA: Academic, 2015, Ch. 17, pp. 907–1000, doi: 10.1016/B978-0-12-382038-9.00017-X.
[99] M. D. Plumbley, A. Cichocki, and R. Bro, "Non-negative mixtures," in *Handbook of Blind Source Separation*, P. Comon and C. Jutten, Eds. Oxford, U.K.: Academic, 2010, Ch. 13, pp. 515–547. [Online]. Available: https://doi.org/10.1016/B978-0-12-374726-6.00018-7
[100] A. P. Piotrowski, J. J. Napiorkowski, and A. E. Piotrowska, "Population size in particle swarm optimization," *Swarm Evol. Comput.*, vol. 58, Nov. 2020, Art. no. 100718, doi: 10.1016/j.swevo.2020.100718.
[101] D. Karaboga and B. Basturk, "Artificial bee colony (ABC) optimization algorithm for solving constrained optimization problems," in *Foundations of Fuzzy Logic and Soft Computing*. Berlin, Germany: Springer,2007, pp. 789–798.
[102] E. Schulz, M. Speekenbrik, and A. Krause, "A tutorial on Gaussian process regression: Modelling, exploring, and exploiting functions," *J. Math. Psychol.*, vol. 85, pp. 1–16, Aug. 2018.

AMAN KUMAR was born in Bilaspur, Himachal Pradesh, India. He received the Master of Engineering degree in construction technology and management from the National Institute of Technical Teacher's Training and Research Institute, Chandigarh, India. He is currently pursuing the Ph.D. degree in engineering sciences (structural engineering) with the CSIR-Central Building Research Institute, Roorkee, India. His research interests include sustainability development, non-destructive testing, concrete technology, strengthening techniques (FRP and FRCM), corrosion protection techniques for structural design, artificial intelligence and the Internet of Things (IoT). He has carried out a great deal of research and technical survey work and has performed several studies in the above-mentioned areas. He has written book chapters and research papers which have been published in scientific international books and journals.

HARISH CHANDRA ARORA received the master's and Ph.D. degrees in structural engineering from the Indian Institute of Technology (IIT), Roorkee, Uttarakhand, India. He is currently working as the Principal Scientist with the Structural Engineering Group, CSIR-Central Building Research Institute, Roorkee, Uttarakhand. He has an experience of more than 25 years in the field of research and development. His research interests include concrete technology, distress diagnosis and repair, and rehabilitation of structures. His research works have been credited in national as well as international journals. He has guided more than 100 students for Bachelor of Technology and Masters of Technology programs. He is also supervising two research scholars for their doctoral programs at the Central Building Research Institute Roorkee.

MAZIN ABED MOHAMMED received the B.Sc. degree in computer science from the University of Anbar, Iraq, in 2008, the M.Sc. degree in information technology from UNITEN, Malaysia, in 2011, and the Ph.D. degree in information technology from UTeM, Malaysia, in 2019. He is currently a Lecturer with the College of Computer Science and Information Technology, University of Anbar, Iraq. His research interests include artificial intelligence, biomedical computing, and optimization.

KRISHNA KUMAR (Graduate Student Member, IEEE) received the B.E. degree in electronics and communication engineering from the Govind Ballabh Pant Engineering College, Pauri Garhwal, and the M.Tech. degree in digital systems from Motilal Nehru NIT Allahabad. He is currently pursuing the Ph.D. degree with the Indian Institute of Technology, Roorkee. He is currently working as a Research and Development Engineer at UJVN Ltd. Before joining UJVNL, he has worked as an Assistant Professor at BTKIT, Dwarahat. He has more than 11 years of experience and has published numerous research papers in international journals, such as IEEE, Elsevier, Taylor and Francis, Springer, and Wiley. His research interests include renewable energy and artificial intelligence.

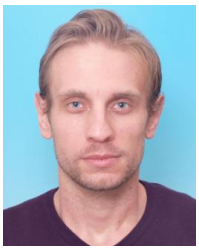

JAN NEDOMA (Senior Member, IEEE) was born in Czech Republic, in 1988. He received the master's degree in information and communication technology from the Technical University of Ostrava, in 2014. Since 2014, he has been working with the Technical University of Ostrava as a Research Fellow. In 2018, he successfully defended his dissertation thesis and he started working as an Assistant Professor with the Technical University of Ostrava. He has become an Associate Professor in communication technologies, in 2021, after defending the habilitation thesis titled "Fiber-optic sensors in biomedicine: Monitoring of vital functions of the human body in Magnetic Resonance (MR) environment" and become the Head of the Optoelectronics Laboratory. He has more than 150 journal articles and conference papers in his research areas and nine valid patents, such as IEEE Reviews in *Biomedical Engineering*, IEEE TRANSACTIONS ON INSTRUMENTATION AND MEASUREMENT, IEEE ACCESS, *Human-Centric Computing and Information Sciences*, and *Frontiers in Physiology*. His research interests include optical communications, optical atmospheric communications, optoelectronics, optical measurements, measurements in telecommunication technology, fiber-optic sensory systems, biomedical engineering, data processing from fiber-optic sensors, the use of fiber-optic sensors within the SMART technological concepts (smart home, smart home care, intelligent building, smart grids, smart metering, and smart cities), and for the needs of industry 4.0.